

Integrated Oxyfuel Power Plant with Improved CO₂ Separation and Compression Technology for EOR application

Item Type	Article
Authors	Font Palma, Carolina;Errey, Olivia;Corden, Caroline;Chalmers, Hannah;Lucquiaud, Mathieu;Sanchez del Rio, Maria;Jackson, Steve;Medcalf, Daniel;Livesey, Bryony;Gibbins, Jon;Pourkashanian, Mohamed
Citation	Font-Palma, C., Errey, O., Corden, C., Chalmers, H., Lucquiaud, M., Sanchez del Rio, M., . . . Pourkashanian, M. (2016). Integrated oxyfuel power plant with improved CO ₂ separation and compression technology for EOR application. <i>Process Safety and Environmental Protection</i> , 103, Part B, 455-465. http://dx.doi.org/10.1016/j.psep.2016.06.024
DOI	10.1016/j.psep.2016.06.024
Publisher	Elsevier
Journal	Process Safety and Environmental Protection
Download date	2026-05-12 06:20:55
Item License	http://creativecommons.org/licenses/by-nc-nd/4.0/
Link to Item	http://hdl.handle.net/10034/614890

Integrated Oxyfuel Power Plant with Improved CO₂ Separation and Compression Technology for EOR application

C. Font-Palma^{a,1,*}, O. Errey^b, C. Corden^c, H. Chalmers^b, M. Lucquiaud^b, M. Sanchez del Rio^b, S. Jackson^c, D. Medcalf^c, B. Livesey^c, J. Gibbins^{b,2}, and M. Pourkashanian^{a,2}

^a*Energy Technology and Innovation Initiative (ETII), University of Leeds, Leeds, LS2 9JT, UK*

^b*School of Engineering, University of Edinburgh, Edinburgh, EH9 3JL, UK*

^c*Costain Natural Resources Division, 1500 Aviator Way, Manchester Business Park, Manchester, M22 5TG*

Abstract

An integrated advanced supercritical coal-fired oxyfuel power plant with a novel cryogenic CO₂ separation and compression technology for high purity CO₂ to suit injection for enhanced oil recovery purposes is investigated. The full process is modelled in Aspen Plus® consisting of: an Air Separation Unit (ASU), an Advanced Supercritical Pulverised Fuel (ASC PF) power plant with a bituminous coal as feedstock, a steam cycle, and a Carbon dioxide Purification Unit (CPU). The proposed CPU process accommodates a distillation column with an integrated reboiler duty to achieve a very high purity CO₂ product (99.9%) with constrained oxygen levels (100 ppm). This work presents a detailed analysis of the CO₂ separation and compression process within the full power plant, including effective heat integration to reduce the electricity output penalty associated with oxyfuel CO₂ capture. The results of this analysis are compared with previous studies and indicate that the combined application of process optimisation in the CPU and advanced heat integration with the power plant offer promising results: In this work a high purity CO₂ product was achieved while maintaining 90% capture for a net plant efficiency of 38.02% (LHV), compared with a thermal efficiency of 37.76% (LHV) for a reference simulation of an ASC PF oxy-fired plant with advanced heat integration, providing a lower purity CO₂ product.

Keywords: oxyfuel combustion, Carbon dioxide Purification Unit, heat integration, enhanced oil recovery

**Corresponding author: c.fontpalma@chester.ac.uk, c.fontpalma@gmail.com*

Present address: ¹Department of Chemical Engineering, University of Chester, Chester, CH2 4NU, UK

²Energy 2050, Energy Engineering group, University of Sheffield, Sheffield, S10 2TN, UK

1. Introduction

Oxyfuel combustion, the combustion of fuels in an oxygen rich mixture, produces a flue gas stream consisting predominantly of carbon dioxide (CO₂) and water, with additional contaminants (including N₂, Ar, O₂, SO_x, NO_x) present at much lower concentrations than in air fired combustion. This flue gas can be further processed to obtain a high purity CO₂ stream. Oxyfuel combustion for power generation was proposed as a solution in the early 1980s for two emerging complementary needs: the reduction of greenhouse gas emissions from fossil fuel energy production, and the production of a high-purity CO₂ stream for utilisation in Enhanced Oil Recovery (EOR) (Boot-Handford et al., 2014). Several pilot scale studies and demonstration projects of oxyfuel power generation technologies for CO₂ capture purposes have since been successfully undertaken, such as Vattenfall's 30 MW_{th} pilot plant at Schwarze Pumpe in Germany, Total's 30 MW_{th} Lacq project with a 27 km pipeline for CO₂ to the Rousse reservoir in France, 30 MW_e Callide oxy-fuel project in Australia, and CIUDEN 30 MW_{th} CFB project in Spain (Wall et al., 2011).

CO₂-EOR employs CO₂ in depleted oil and gas reservoirs to increase production. CO₂-EOR additionally offers a method for CO₂ sequestration, as a significant proportion (40-60%) of the CO₂ injected in oil reservoirs typically remains geologically retained, whilst the rest can be recycled after its separation from oil, with the possibility of being stored after reinjection (Abbas et al., 2013). CO₂-EOR has been extensively applied: by May 2014, 136 EOR projects using CO₂ floods provided 305,710 barrels per day of incremental oil production in the U.S, and 15 CO₂-EOR projects accounted for an additional 35,913 barrels per day in the rest of the world (Koottungal, 2014). The CO₂-EOR worldwide potential has been estimated as 370 billion metric tons based on the CO₂ demand of large oil fields located within 800 km of large CO₂ emitting facilities (Kuuskraa, 2013). By 2014, approximately 6000 km of pipeline infrastructure existed, mainly located in the US and Canada, enabling the transportation of CO₂ to sites for EOR applications (Boot-Handford et al., 2014).

An important consideration for oxyfuel combustion processes with CO₂ capture is the economic reduction of impurities in the CO₂ stream to concentration levels that comply with environmental and legal requirements (Pipitone and Bolland, 2009). CO₂ purity levels are generally defined by specifications of CO₂ transport, storage and environmental regulations. In addition, typical EOR operations limit CO₂ impurity concentrations by the specification that CO₂ should dissolve in oil at the temperature and pressure conditions of the oil reservoir.

This is measured by the minimum miscibility pressure (MMP), which is the minimum pressure at which an injection gas can achieve multiple-contact miscibility with the reservoir oil. To maintain the MMP with oil, the amount of impurities in the CO₂ stream should be controlled, e.g. O₂, N₂, Ar, H₂ and CO are immiscible with oil and increase the MMP, whilst H₂S, SO₂, and C₂H₆ decrease the MMP (de Visser et al., 2008).

Table 1 shows specifications set by industry for the flue gas (CO₂) composition after purification. The differences are due to case specific recommendations for CO₂ quality for pipeline transportation based on business guidelines or agreements between the CO₂ producer and the transporter (de Visser et al., 2008). The limits shown in Table 1 have been stipulated according to different criteria relevant to the impurity. The water content is restricted to avoid the occurrence of corrosion, and free water and hydrate formations; the limits of H₂S in CO₂ are set based on health and safety considerations due to its high toxicity; and non-condensable gases (N₂, H₂ and Ar) concentrations are limited for design and operational reasons. It should be noted that studies typically suggest that acceptable levels of O₂ in CO₂ are substantially lower for CO₂ to be used in EOR operations than for CO₂ to be stored in other geological formations. Although there is a lack of fundamental research on the allowable concentration of O₂ in CO₂, limits have been recommended based on several concerns, such as potential exothermal reactions with oil that can cause overheating in the injection point, increased biological growth and the higher viscosity of oxidised oil which raises extraction costs (de Visser et al., 2007). The presence of impurities with lower critical temperatures and pressures than CO₂, such as H₂ or N₂, will promote pressure and temperature drops along a set pipeline length (Serpa et al., 2011). An increase in pressure drop could require more booster stations at shorter intervals to keep the pressure sufficiently high to maintain a dense-phase flow (Boot-Handford et al., 2014). Table 1 reports a total of 4 % for non-condensables (N₂, O₂, H₂, CH₄ and Ar) for the Dynamis programme based on safety limits, infrastructure durability and compression work. It should be noted that in addition to the values reported in Table 1, a recent report specific to the effects of impurities on the hydraulic design of CO₂ transport networks suggests that total impurities of up to 2 % in the CO₂ product stream should perhaps be targeted to minimise the impact on pipeline costs (Wetenhall et al., 2014).

Table 1 Review of specifications for CO₂-containing stream leaving the boundary of the plant after purification

Component	Canyon Reef project (Metz et al., 2005)	Weyburn pipeline (Metz et al., 2005)	Gullfaks (Pipitone and Bolland, 2009)	US pipeline specifications (Posch and Haider, 2012)	DYNAMIS programme (de Visser et al., 2007)	DOE/NETL (DOE/NETL, 2012)
EOR or aquifer	EOR	EOR	EOR	EOR	Both	Both
CO ₂	> 95%	96%	99.5%	> 95%	> 95.5%	> 95%
Ar	-	-	-	-	< 4% ^a	1% (EOR) ^a 4% (aquifer) ^a
CO	-	0.1%	< 10 ppm	-	2000 ppm	35 ppm
H ₂ O	No free water < 0.489 g Nm ⁻³ in vapour phase	< 20 ppm	H ₂ O vapour content equivalent to saturation at -5°C	0.4805 g Nm ⁻³	500 ppm	500 ppm
H ₂ S	< 1500 ppm (wt.)	0.9%	-	10 -200 ppm	200 ppm	0.01%
SO _x	-	-	< 10 ppm	-	100 ppm	100 ppm
Total sulfur	< 1450 ppm (wt.)	-	-	-	-	-
N ₂	< 4% ^a	< 300 ppm	< 0.48%	< 4% ^a	< 4% ^a	1% (EOR) ^a 4% (aquifer) ^a
NO _x	-	-	< 50 ppm	-	100 ppm	100 ppm
O ₂	< 10 ppm (wt.)	< 50 ppm	< 10 ppm	< 10 ppm	100–1000 ppm (EOR) < 4% (aquifer) ^a	0.001%
Glycol	< 4x10 ⁻⁵ Lm ⁻³	-	-	-	-	46 ppb
CH ₄	-	0.7%	-	-	< 2% (EOR) < 4% (aquifer) ^a	1% (EOR) ^a 4% (aquifer) ^a
H ₂	-	-	-	-	< 4% ^a	1% (EOR) ^a 4% (aquifer) ^a
C ₂ + C _x H _y	< 5%	2.3%	100 ppm	< 5%	-	-
Temperature	< 48.9°C	-	-	< 50°C	-	-
Pressure	-	15.2 MPa	-	-	-	-

^a Total for all non-condensable gases < 4 %

The purity level of CO₂ derived from oxy-combustion flue gas is generally not limited by technical barriers but by associated increased capital and operating costs at plant level,

particularly the additional energy requirement involved, which ultimately causes a reduction of power plant electrical output and revenue. This work presents a CO₂ processing scheme integrated with an oxyfuel combustion power plant that provides EOR grade high purity CO₂ at reduced net plant efficiency penalties compared to previous reports.

Various process configurations able to deliver high CO₂ purities have been reported. For example, Strube and Manfrida (2011) carried out process modelling studies on a number of cryogenic CO₂ purification units based on patent applications using Aspen Plus; their aim was to investigate the effect of CO₂ capture on power plant efficiency. The study concluded that, of the designs assessed, the only purification options able to sufficiently reduce impurities for EOR requirements employed integrated distillation (stripping) columns. In other studies, some reported systems employ external refrigeration (for example two refrigeration loops employing ethane and propane (Pipitone and Bolland, 2009), or an external ammonia cooling cycle (Posch and Haider, 2012)) to provide the cooling and heat duty needed in the condenser and reboiler the distillation column, in order to achieve the desired high CO₂ purity and recovery.

This work presents an improved CO₂ separation and compression process, where separation occurs at elevated pressure and low temperatures are achieved through auto refrigeration (Joule-Thomson effect) provided by the evaporation of low-pressure product streams. No external refrigeration is therefore required. A further aspect of the process presented in this analysis is the evaluation of the CO₂ separation and compression process within the full power plant, where the outcome of a comprehensive heat integration study is presented to maximise net plant efficiency. The integrated system is described and compared with previous studies based on performance parameters including CO₂ purity, Carbon dioxide Purification Unit (CPU) power consumption, and electricity output penalty.

2. Methodology

An integrated model of an Advanced Supercritical Pulverised Fuel (ASC PF) power plant operating oxyfuel combustion was developed to assess the penalties imposed by the addition of a novel low temperature CPU for CO₂ capture. In particular, the auto refrigeration process presented for the CPU is designed to provide high purity CO₂ with lower energy penalties. Through the combined application of process optimisation in the CPU and advanced heat integration with the power plant, this study provides an illustration of the potential for reduced energy penalties in oxyfuel processes operating with CO₂ capture for EOR.

The reference case for this study, described in Corden et al. (2014), is based on a report commissioned by the International Energy Agency Greenhouse Gas R&D Programme (IEAGHG) – *Oxy Combustion Processes for CO₂ Capture from Power Plant, Report 2005/9* (Dillon et al., 2005), with Case 2 (ASC PF Power Plant with CO₂ Capture) used as the starting point for this work. Oxyfuel combustion can be applied to different fuel types, but oxy-coal combustion for power generation with CO₂ capture has received more attention due to coal abundance and reliability of supply, the higher carbon content of the coal and the fact that standard coal combustor and steam turbine technologies do not require extensive technology changes for oxy-coal applications.

Power plant simulations were created in Aspen Plus® V8 and initially validated by replicating the boiler, steam cycle and integrated CPU from IEAGHG 2005/9 Case 2. Following review, a number of modifications to this IEAGHG 2005/9 reference case were made and a comparable base case with a LHV efficiency of 37.76% for 90% capture at 95.5 % CO₂ purity was established. The specific changes to the IEAGHG 2005/9 reference are detailed in Corden et al. (2014), and include additional heat sinks in the steam cycle (for gas dehydration in the Air Separation Unit (ASU) and CPU, and for heating vent gases prior to expansion in the CPU) and changes to the steam cycle configuration to better represent typical power plant operation.

In line with the IEAGHG 2005/9 study, this work assumes the absence of a flue gas desulfurisation unit (FGD) for the low sulfur coal reference fuel, with the assumption that NO_x and SO_x will be removed from the exit CO₂ stream during flue gas compression (White et al., 2013). This eliminates any implied direct efficiency losses from the FGD unit, and also allows for the use of flue gas feedwater heaters in the steam cycle, which would not be possible at the cooled outlet of a wet FGD unit. The absence of a FGD alongside advanced heat integration between the steam cycle and other sections of the power plant contribute to a high baseline efficiency from which to integrate the novel CPU.

Simulations were developed for the novel CPU configuration, with improved heat integration between the hot steam cycle and the cold CPU and ASU processes. The model, illustrated in Figure 1, is composed of an ASC PF power plant with a bituminous coal feedstock, a regenerative Rankine steam cycle with a single reheat stage, an ASU and a low temperature CPU.

A constant fuel input of 1502 MW_{th} was used consistent with the IEAGHG 2005/9 Case 2. The model was designed for a CO₂ recovery rate of 90% and CO₂ purity above 99.9%. The modelling details of each section are described further below and Table 2 provides the property methods used in the Aspen Plus model for each section.

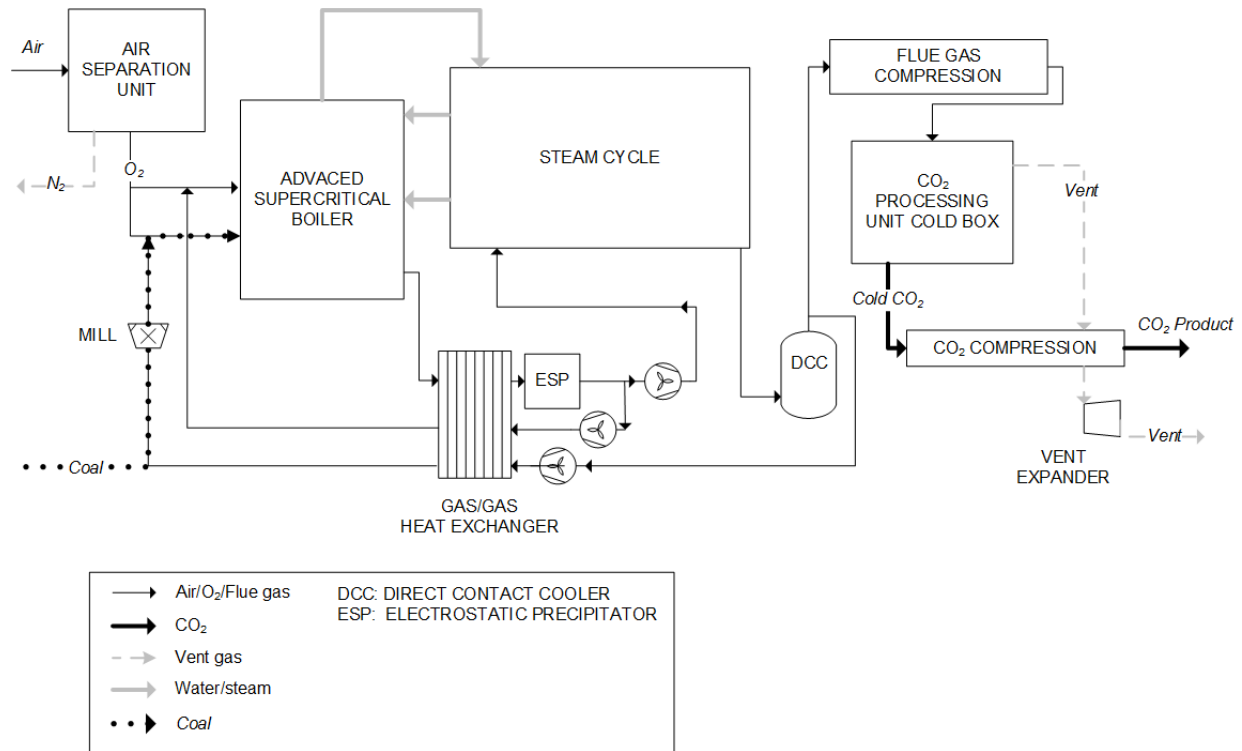


Figure 1 Schematic of the integrated oxyfuel combustion power plant

Table 2 Property methods used in the Aspen Plus model

Fluid	Property Method
Steam/water in steam cycle and boiler	NBS/NRC steam tables
Flue gas in boiler and hot (gas) side of flue gas Feed Water Heater (FWH)	Peng-Robinson equation of state with Boston-Mathias modifications (PR-BM)
Air in ASU	Peng-Robinson equation of state (PR)
Flue gas in CPU and hot (gas) side of FWHs supplying heat to the steam cycle from the CPU	Redlich-Kwong equation of state with the Soave modification (SRK)

2.1 Supercritical boiler

A single reference low sulfur coal has been considered as the fuel in this study, as described in IEAGHG 2005/9. Coal is considered an unconventional solid in Aspen Plus. As a result, the combustion process needs to be divided into two component sub-processes, as in Font Palma and Martin (2013):

i) Devolatilisation of coal: where coal is broken into its constituent elements, ash and energy based on its ultimate analysis, proximate analysis and lower heating value (LHV). This stage uses a reactor modelled by a RYield block.

ii) Combustion reactions: These are based on chemical equilibrium. The temperature and composition of flue gas are estimated through minimisation of the Gibbs free energy using a RGibbs block, wherein product gases are specified, e.g. CO₂, H₂O, O₂, N₂, Ar, NO, NO₂, SO₂, and HCl.

The boiler is modelled using a series of heat exchangers to represent the radiant furnace chamber (HXFlux block), superheater, reheater and economiser (HeatX blocks).

2.2 Air separation unit (ASU)

A cryogenic ASU is used to provide the 95% purity oxygen to the boiler. For study purposes, the three-column system reported in IEAGHG 2005/9 was substituted with a more conventional 2-column system. A small impact on the simulated CPU feed gas composition was observed, but overall results reflected the performance of the cases studied. Since this work involved a full integration of the plant, the main interest was to replicate the intercooling duty of the air compressors, which provided heat for feed water heating as explained below. The basis for heat integration was therefore maintained as 55.3 MW, in accordance with the IEAGHG 2005/9 ASU. ASU compression power requirements were also kept constant.

2.3 Steam cycle

The steam cycle consists of a regenerative Rankine cycle with a single reheat stage and a backwards cascade feedwater heating configuration. Boiler feed water is heated in conventional steam cycle stages using heat from condensing steam exiting the high, intermediate and low pressure turbines. The integrated plant uses heat from other sources in the oxyfuel process for feedwater heating, which either replaces or operates in parallel with

low pressure conventional feedwater heater stages, to reduce the flow rate of steam bleeds. Figure 2 shows a schematic diagram representing key features of the final integrated steam cycle configuration. Increased plant thermal efficiency is achieved through integration of the steam cycle with flue gas heat (FGHTX1 and FGHTX2 in Figure 2) and with heat available from compression intercooling in the ASU and the CPU (ASU HTX1, CPU HTX1-4). Steam is extracted from the cycle to supply high temperature heat to the CPU (CPU HTX5-7 in Figure 2) and low temperature heat to the ASU (ASU HTX2 in Figure 2). As illustrated, there are 5 feedwater heating stages considered in the regenerative cycle, consistent with IEAGHG 2005/9. This is described further in Section 2.5.

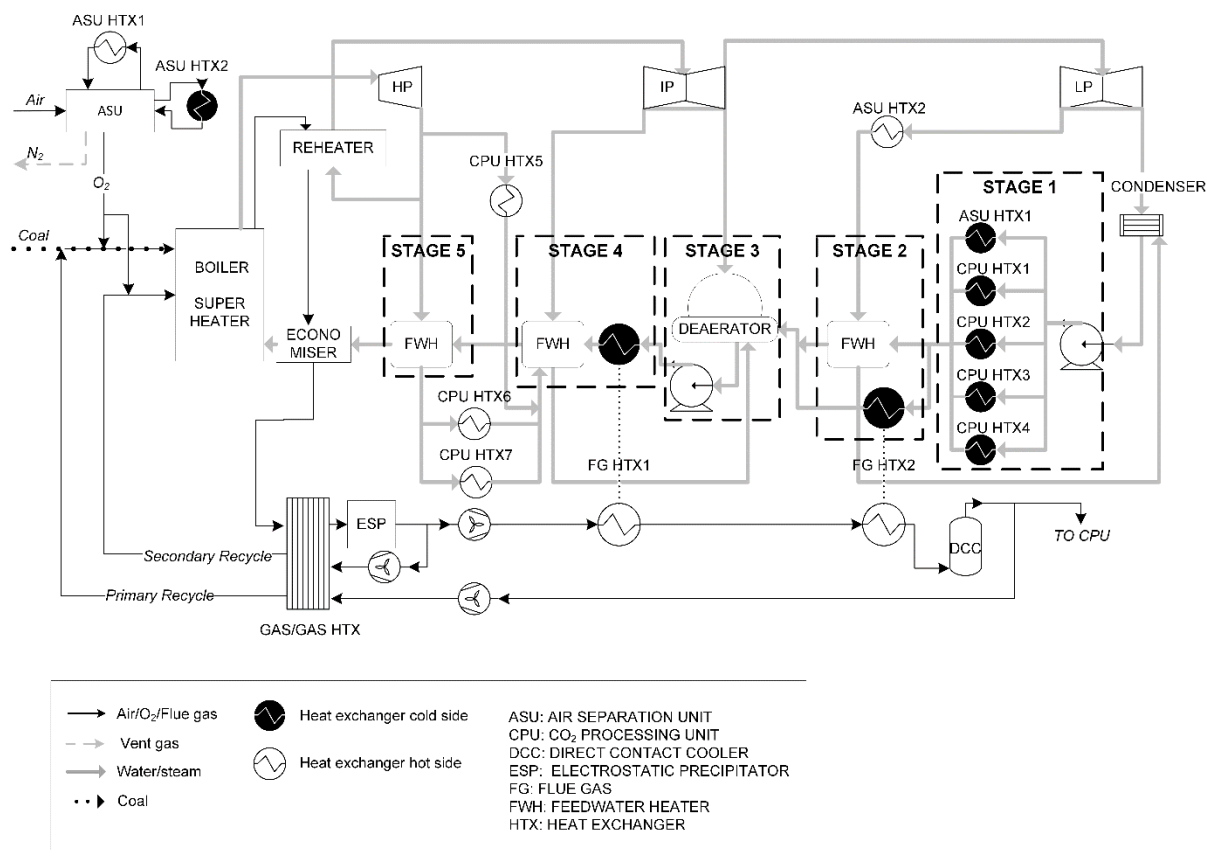


Figure 2 Schematic of integrated oxyfuel plant steam cycle showing heat exchangers (cold and hot side) included in the final design

Steam conditions, steam extraction pressures and turbine efficiencies are provided in Table 3. Turbine isentropic efficiencies were chosen to be consistent with the mass and enthalpy balances taken from the IEAGHG 2005/9 report. Other relevant steam turbine extraction conditions were determined by the outcome of the heat integration, as detailed in Section 2.5.

Table 3 Steam cycle modelling parameters

High pressure (HP) steam	
Superheated steam pressure	290.0 bara
Superheated steam temperature	600.0°C
HP turbine efficiency	87.4 %
Intermediate pressure (IP) steam	
Reheated steam pressure	61.1 bara
Reheated steam temperature	620.0°C
IP steam turbine efficiency - First group of stages	91.2 %
IP steam turbine efficiency - Second group of stages	92.0 %
Low pressure (LP) steam	
LP steam turbine efficiency - First group of stages	91.83 %
LP steam turbine efficiency - Second group of stages	87.0 %
LP steam exit extraction pressure - Condenser inlet	0.04 bara
LP steam exit extraction temperature - Condenser inlet	29.1°C
Feedwater	
Condensate pressure after condensate pump	16.0 bara
Condensate temperature after condensate pump	29.1°C
Feedwater exit pressure to economiser inlet	328.6 bara
Feedwater exit temperature to economiser inlet	270.3°C
Mass balance around steam cycle	
Superheated steam flow to HP turbine	516 kg/s
HP turbine steam losses	3 kg/s
Make up to condenser	11 kg/s
Feedwater flow to boiler	524 kg/s

Feedwater heaters were modelled as countercurrent, assuming full condensation of the steam stream and a temperature difference between the saturation temperature of the steam and the exit temperature of the boiler feedwater of 0.5°C, accounting for superheat. All feedwater heater condensate streams are assumed to be subcooled to 10°C above the temperature of the

entering feedwater. These temperature differences are achieved through controlling the flowrate of condensing steam through the feedwater heater. An exception is the last feedwater heater before the economiser (heated by steam exiting the HP turbine), where the temperature difference is constrained by the economiser feedwater inlet temperature and the HP steam pressure, both maintained from the original IEAGHG 2005/9 report to replicate boiler conditions. In this case the terminal difference between the boiler feedwater exit (entering the economiser) and the HP steam saturation temperature is 10°C.

The deaerator was modelled as a Mixer block, with an exit temperature equal to the saturation temperature of the inlet steam stream. This mixer is followed by a heater to ensure a vapour fraction of zero, controlled by the flowrate of the inlet steam bleed.

Pinch temperatures and pressure drops are set to provide direct comparison with IEAGHG 2005/9 and are summarised in Table 4.

Table 4 Steam cycle heat exchanger modelling parameters

Pressure drops	bar
Water side pressure drop across feedwater heaters	3.3
Cooling water pressure drop across the condenser	3.3
Temperature pinch/approaches	°C
Water temperature rise after pinch in feedwater heaters (terminal difference)	<1
Hot side condensate drain from feedwater heater and cold side inlet temperature	10
Temperature approach for flue gas feedwater heat exchangers	25

2.4 Carbon Dioxide Purification Unit (CPU)

In this work, NO_x and SO_x levels are assumed to be entirely removed after flue gas compression, based on a patented method by Air Products (Allam, 2008 described in White et al., 2013) for the removal of gas contaminants. In particular, SO₂, NO_x, and Hg, can be removed during the flue gas compression train by reactive distillation prior to the cryogenic CO₂ purification. This approach enables direct comparison against IEAGHG 2005/9.

Based on the Air Products method outlined above, the study configuration for flue gas compression includes the provision of two water wash stages, at approximately 15 and 30 bar in which NO and SO₂ are oxidised and converted to nitric acid and sulfuric acid, respectively.

After the second wash stage, 95% of the NO is converted and removed as acid, whilst the conversion rate for SO₂ is 99.5% (Allam, 2008; White et al., 2013). For this study, NO_x and SO_x removal was not modelled in detail.

In the low temperature CPU process, CO₂ purification is achieved by one or more stages of partial condensation and separation of the resulting vapour and liquid phases. The required purity and recovery is accomplished by adjustment of operating temperatures and pressures. As temperatures are reduced, the quantity of O₂/Ar/N₂ components in the liquid phases of the CPU process increases and CO₂ purity is reduced. At the same time, the absolute recovery of CO₂ in the liquid phase is increased. The operating pressure similarly affects both purity and recovery, with increasing pressure reducing purity but increasing recovery. Thus, the selection of operating temperatures and pressures becomes a compromise, wherein high recovery is reached for low temperatures and high pressures. Operating temperatures are limited by the freezing point of CO₂ (the triple point temperature of CO₂ is -56.6°C). Purity can be further increased by the introduction of additional flash separation stages in the liquid systems – to remove the lower boiling point O₂/N₂/Ar components, as previously reported (Besong et al., 2013; Corden et al., 2012). For an EOR grade high purity CO₂ product, multiple further separation stages are required, provided within a stripping column.

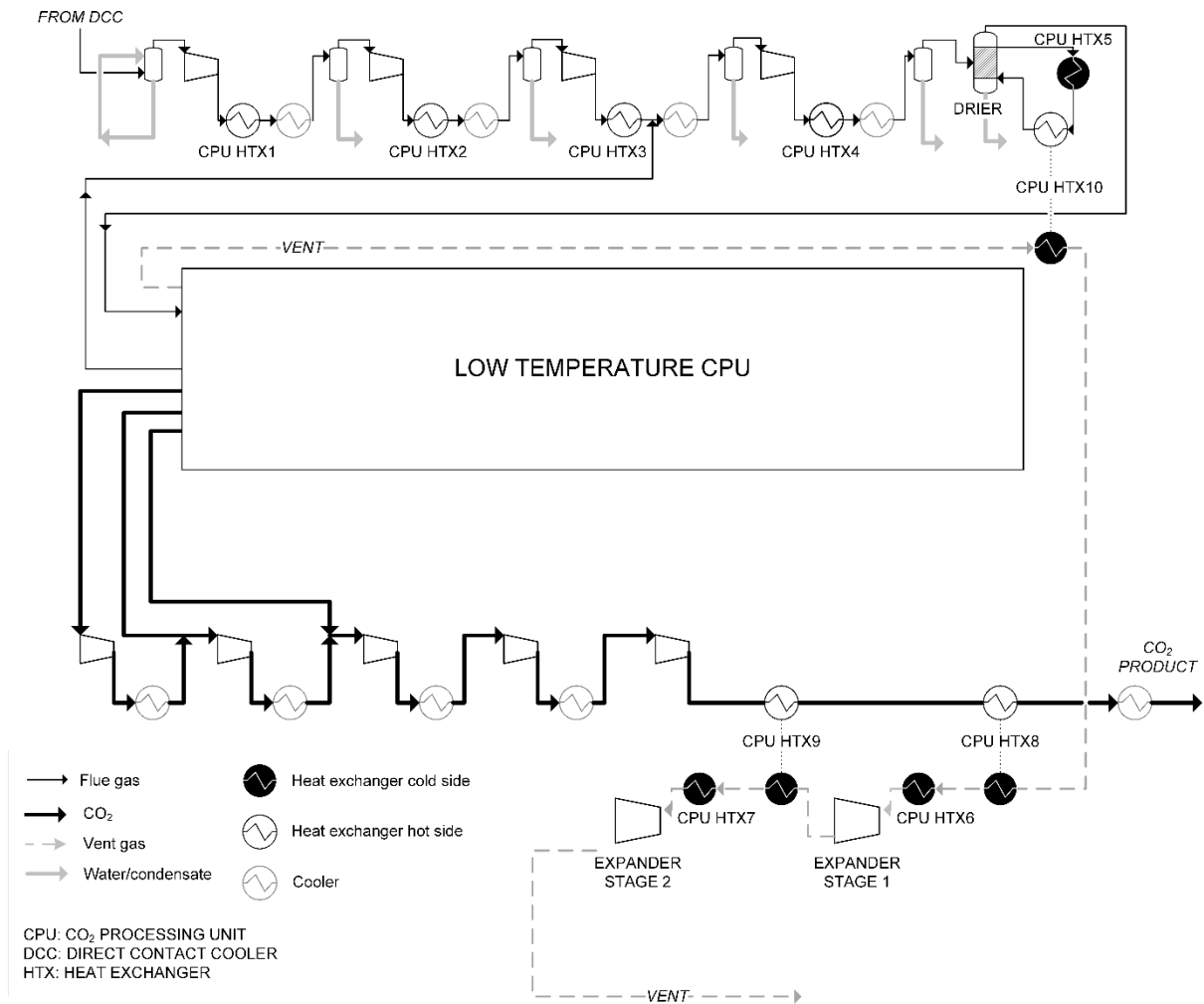


Figure 3 Schematic process flow diagram of CPU: High purity column with product split scheme

The high purity liquid CO₂ product from the column is split to provide more optimal cooling at maximised pressure levels, before being directed to the product gas compressor at three different, pressure matched stages. The overhead vapour of the second flash separator contains inerts with a low CO₂ concentration, which are vented to the atmosphere via a power generating expander system.

Figure 3 also shows the proposed compressor configuration, which has four and five compression stages for the flue gas and CO₂ compression, respectively. Inter-cooling between stages was set at 20°C and compressor polytropic efficiencies at 85%, consistent with the reference IEAGHG 2005/9 study. Compared with the IEAGHG 2005/9 base case, the CPU configuration used in this work has a relatively large number of compression stages.

The current study compressor configuration reduces power requirements (see Table 6) by restricting the maximum operating/discharge temperature to 150°C between stages but, compared to the IEAGHG reference case that uses discharge temperatures of up to 300°C, also reduces the temperature at which heat is available for integration with other processes.

2.5 Heat integration

Heat integration is carried out between the steam cycle and other hot and cold streams in the oxy-combustion plant. The following section outlines the approach taken considering the cold and hot process streams, summarised in Table 5.

Cold streams: There are four cold streams (requiring heat) considered in the heat integration. The major cold stream is the boiler feedwater that exits the condenser at 29°C. It is progressively heated through a series of feedwater heaters and then enters the boiler economiser at 270°C. These temperatures follow IEAGHG 2005/9 assumptions of cooling water and boiler operation. Additional cold streams are within the temperature swing gas dehydration processes in the ASU and CPU (with heat addition occurring in ASU HTX2 and CPU HTX5) and the pressurised vent gas stream that leaves the CPU (heated in CPU HTX6 and CPU HTX7 in Figure 2 and Figure 3). The motivation for heating the vent gas is power recovery, where expansion of the inert gases vented to the atmosphere is exploited. The inert gases must be heated prior to the turbine in order to ensure good dispersion to the atmosphere at the outlet of the turbine.

Hot streams: The hot (to be cooled) streams considered are the boiler flue gases exiting the electrostatic precipitator, which are cooled to the acid dew point providing heat in FG HTX1 and FG HTX2 in Figure 2, and the hot gas at compression intercooling stages in both the ASU (ASU HTX1 in Figure 2) and the CPU (CPU HTX1-4 and CPU HTX8-9 in Figure 3). Compression intercooling was set to reduce the temperature of gases entering compressors to 20°C. The final CO₂ product exit stream is cooled to 40°C to remain above the critical point at high pressure.

The available heat duty for integration after discounting excess low grade heat and taking account of heat exchanger pinch limits is summarized in Table 5.

Table 5 Summary of process hot and cold streams integrated with the steam cycle

	Supply temperature (°C)	Target temperature (°C)	Heat capacity flow rate (kW/°C)	Heat duty (MW)
Streams to be cooled (hot streams)				
ASU compressor inter/after cooler duty	144	20	446	55.3
CPU compressor inter/after cooler duty	81-106	20	690	53.0
Flue gas heat exchange	224	121	365	37.6
<i>TOTAL</i>				145.9
Streams requiring heat (cold streams)				
Boiler feedwater	29	270	1291	311.2
CPU drier regeneration	20	240	6	1.4
ASU drier regeneration	20	170	47	7.0
Vent heat	3	150	81	11.9
<i>TOTAL</i>				331.5

Heat available from the hot streams was integrated with the steam cycle through heat exchangers configured either “in parallel” or “in series” along the main boiler feedwater stream in order to minimize the maximum temperature difference in the heat exchangers and maximize the integration efficiency. Additional heat is taken from condensing superheated steam extracted from the high, intermediate and low pressure turbines.

As illustrated in Figure 2, this work considers five stages of feedwater heating, consistent with the base case. Figure 2 also shows the final design and location of the proposed heat exchangers that integrate hot and cold sources. The new five stages consist of:

- i) Stage 1 is heated wholly by heat sources external to the steam cycle, using low grade heat from the CPU and ASU. Figure 3 shows the CPU heat sources used for feedwater heating with the heat exchangers labelled with the same names as in Figure 2 (CPU HTX1-4);

- ii) Stage 2 uses a low pressure feedwater heater in parallel with heat from boiler flue gas;
- iii) Stage 3 comprises the deaerator and deaerator pump heated by steam exiting the IP turbine;
- iv) Stage 4 gains heat from hot boiler flue gas followed by a feedwater heater using steam from a bleed from the IP turbine; and
- v) Stage 5 is a feedwater heater using steam from the HP turbine only.

Cold stream integration is achieved by extracting heat from the steam cycle. Heat for temperature swing dehydration in the ASU and CPU is taken from condensing steam bleeds to meet the temperature requirements assumed in the study. The CPU vent heating duty uses the low grade heat available within the CPU, but requires further heating to reach the required temperatures prior to expansion. To minimise size and cost of heaters, this heat is taken from condensed steam exiting the high pressure feedwater heater.

Heat integration was achieved through an 'equal enthalpy' approach, whereby an equal enthalpy rise is applied to each feedwater heating stage in the steam cycle. This increases the efficiency in a manner that approaches an ideal cycle. In general, the feedwater heating stages are calculated according to the equal enthalpy rise approach with some adjustments as discussed below. In particular, the equal enthalpy approach is not used for stage 1 because it could limit the addition of all the low grade heat available, and is not used for stage 5 because of the constraint of maintaining constant boiler sizing and operations for comparability with the IEAGHG 2005/9 study.

Stage 1: The first feedwater heating stage uses the maximum possible low grade heat, in parallel FWHs, to raise the feed water from 29.1°C to approximately 80°C. Only low grade heat is available from CPU intercooling at 105°C or lower. A 25°C gas-liquid approach is assumed, so the feed water exit temperature will be approximately 80°C. Likewise, the exiting compressed gas temperature will be 54°C, 25°C above the condensate temperature at the outlet of the condensate pump. Further cooling is used in the CPU to reduce the compressed gas temperature to 20°C for the subsequent compressor stage. Additionally, heat from the ASU is supplied to the steam cycle at temperatures that allow feed water to reach temperatures of 84°C, as reported in other studies (Dillon et al, 2005).

Stages 2-4: The heat duty is calculated using an equal enthalpy difference for each stage. This allows for even enthalpy increase across the stages approximating reversible heat addition. The total enthalpy change over stages 2-4 is defined as the sum of the enthalpy change in three streams:

- a) the water exiting stage 1, and entering stage 5;
- b) the condensed water from the IP bleed exiting stage 3, and entering stage 5; and
- c) the water from the IP FWH drain (containing both the HP and IP FWH bleeds) entering stage 3, and entering stage 5.

This total enthalpy change is then divided by 3; the number of stages. The enthalpy change over each stage is defined as follows (Eq. 1):

$$\dot{H}_{stage} = \frac{\dot{H}_{fw,a} + \dot{H}_{fw,b} + \dot{H}_{fw,c}}{N_{stages}} \quad \text{Eq. 1}$$

where,

\dot{H}_{stage} : Enthalpy difference across each feed water heating stage (MW)

$\dot{H}_{fw,a}$: Enthalpy difference in feed water fraction a (MW)

$\dot{H}_{fw,b}$: Enthalpy difference in feed water fraction b (MW)

$\dot{H}_{fw,c}$: Enthalpy difference in feed water fraction c (MW)

N_{stages} : number of stages

Stage 5: This study maintains boiler sizing and operation for consistency with the IEAGHG 2005/9 study. The final stage of heating is constrained by this approach since the flow and conditions of the superheated steam entering the HP turbine remains constant, as does the flow of steam to the reheater and subsequently the IP turbine. This also constrains the steam bleed to stage 5. Similarly, the flow and conditions of the feedwater exiting the final stage to the economiser inlet must also remain constant, with the condensing steam exiting as subcooled water 10°C above the feed water inlet temperature.

A grand composite curve of the integrated process, before the introduction of any turbine steam bleeds, or cooling water is shown in Figure 4. This diagram illustrates the total enthalpy in the integrated system (y-axis) at a given temperature (x-axis). Where the enthalpy is zero, the system can be fully integrated with no requirement for additional utility streams. Where the enthalpy is positive, additional heating or cooling is required. Therefore, the grand composite shows how much heating and cooling is required and at what temperatures it is needed. Below 80°C not all of the heat from compression intercooling can be utilised and additional cooling water is required. Above 80°C additional heating is required, which is taken from turbine bleeds in the steam cycle.

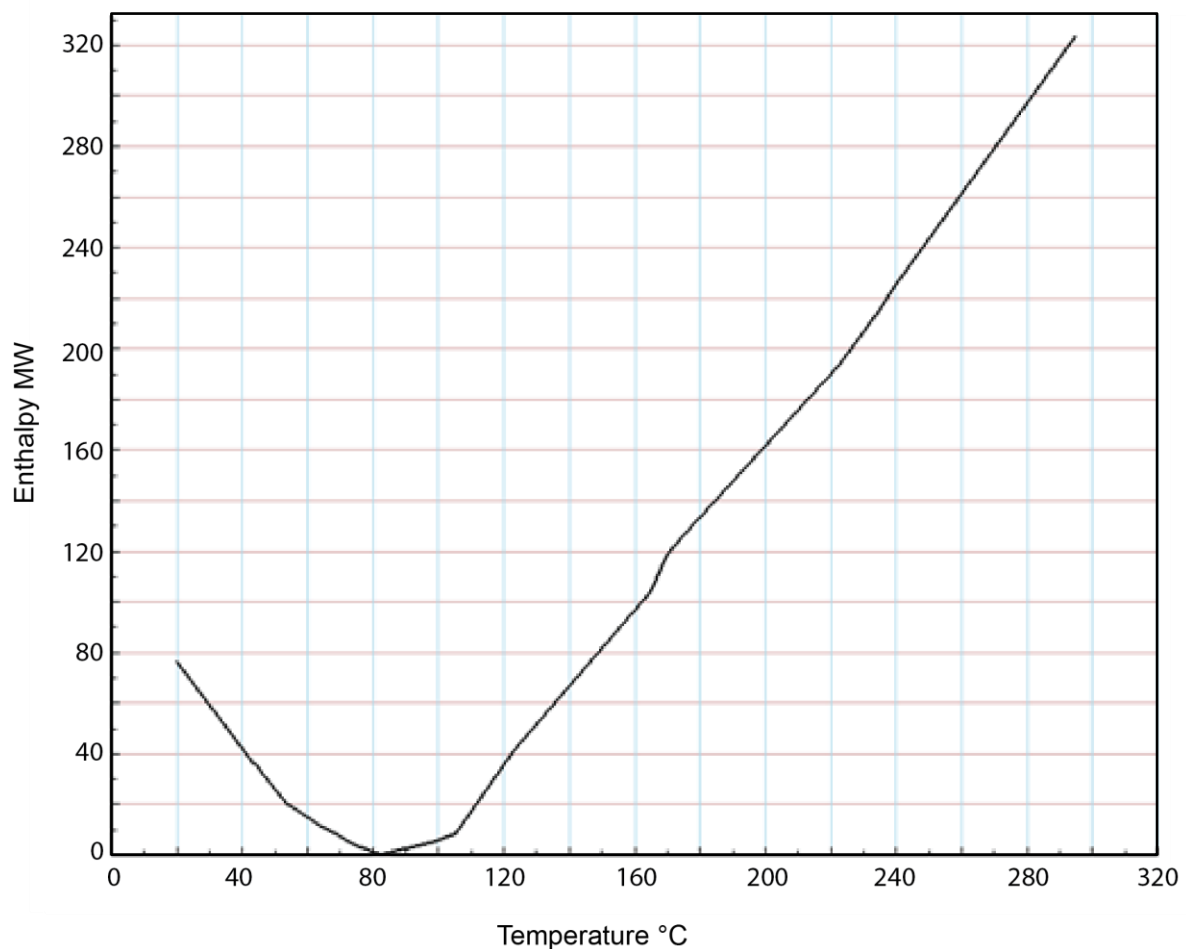


Figure 4 Grand composite curve of hot and cold streams before turbine steam bleeds and cooling water requirements are taken into account

3. Results and Discussion

3.1 CPU performance

This study explores the performance of a CPU, where the high purity liquid CO₂ stream from the bottoms of the distillation column is split to provide optimal cooling at maximised pressure levels, to minimise the power consumption required for recompression in the product gas compressor, as shown in Figure 3.

In this work, CO₂ purity reaches 99.98% with a recovery ratio of 90%, at a net plant efficiency of 38.02% LHV including ASU and CPU penalties. This is slightly higher than the base case that presents a net efficiency of 37.76 % LHV for 90% capture at a CO₂ purity of just 95% with the same nominal superheat and reheat steam temperature and pressure in the boiler. In addition, the power consumption of the CPU is less than those values found in the literature as compared in Table 6.

Table 6 compares configurations of different proposed CO₂ purification processes. The first two columns give the base case and optimized EOR case for the current study. The lower CO₂ purity base case is modelled on the IEAGHG report but revised and evaluated for consistent comparison in this work (Corden et al., 2014). These are contrasted with findings from patented cryogenic CO₂ purification process configurations described and evaluated by Strube and Manfrida (2011) who assessed different configurations, adapted respectively from patent applications by Air Products, Air Liquide and Praxair. The Strube and Manfrida work also references the IEAGHG 2005/9 report but adjustments have resulted in lower baseline power plant efficiencies than the current study. It is assumed that the trends in relative changes can be considered against those of the current work.

The last two columns show the performance of CPU systems evaluated as standalone components (Pipitone and Bolland, 2009; Posch and Haider, 2012).

The studies used for performance comparison in Table 6 are chosen due to their CO₂ purity specifications and relative similarities in fuel specification and process to this work. However, differences in process configurations between the studies, including baseline power plant efficiencies and CO₂ recovery %, dictate that direct comparison between the numerical values is limited and general trends between the performance metrics should be considered more relevant.

As described, while simple flash separation can be used to achieve CO₂ purities suitable for sequestration, a stripping column or distillation process is required to achieve higher purities for EOR.

Table 6 Performance of oxy-fuel power plant with cryogenic CO₂ purification

	Base case	This work	Strube and Manfrida (2011)					Others	
	IEAGHG 2005/9, Air Products ^a	EOR case - Costain	Air Products Base Case	Air Products 17 bar stripping	Air Products 30 bar stripping	Air Liquide	Praxair	Pipitone and Bolland (2009) ^b Case 2	Posch and Haider (2012) ^b Type 2
Flue gas composition after pre-compression and water removal (% mol)									
CO ₂	76.0	76.0	75.3	75.3	75.3	75.3	74.4	75.0	77.4
Ar	3.6	3.6						2.3	3.2
N ₂	14.1	14.1						16.4	11.5
O ₂	5.5	5.5						6.0	7.9
Separation method	Two flash units	Two flash units and stripper	Two flash units	Flash separator and stripper	Two flash separators and stripper	Distillation column, stripper, and flash vessel ^c	Stripper column and flash vessel ^d	Distillation separation	Distillation separation
CO ₂ recovery (%)	90.0	90.0	86.5	86.4	85.7	86.6	82.2	86.9	87.6 – 90.1
Total amount of work in the CPU per kg stored CO ₂ (kJ/kg)	526.8 (146.3 kWh/tCO ₂)	435.23 (120.9 kWh/tCO ₂)	492 (136.7 kWh/tCO ₂)	509 (141.4 kWh/tCO ₂)	627 (174.2 kWh/tCO ₂)	412 (114.4 kWh/tCO ₂)	492 (136.7 kWh/tCO ₂)	602.9 (167.6 kWh/tCO ₂)	700 (195 kWh/tCO ₂)
Product gas composition (% mol)									
CO ₂	95.5%	99.98%	96.1%	99.97%	99.99%	99.99%	99.9%	99.3%	99.99%
O ₂	1.4%	100 ppm	0.73%	176 ppm	46.5 ppm	35.6 ppm	363 ppm	4000 ppm)	6 ppm
Pressure (bar)	110	110	110	110	110	110	110	110	120
Gross power plant output (MW _{el})	785.3	778.2	584.6					596.0	-

	Base case	This work	Strube and Manfrida (2011)					Others	
	IEAGHG 2005/9, Air Products ^a	EOR case - Costain	Air Products Base Case	Air Products 17 bar stripping	Air Products 30 bar stripping	Air Liquide	Praxair	Pipitone and Bolland (2009) ^b Case 2	Posch and Haider (2012) ^b Type 2
Gross plant efficiency (%LHV)	52.3%	51.8%	40.7%					-	-
CPU flue gas compression (MW _{el})	53.9	47.3	50.9	50.9	50.9	39.6	48.0	42.2	
CPU CO ₂ compression (MW _{el})	20.0	15.4	10.5	13.1	25.2	10.7	13.4	28.5	
Net CPU power consumption (MW _{el})	64.9	53.7	51.2	52.9	65	42.8	48.9	70.7	
ASU power consumption (MW _{el})	86.7	86.7	84.6	84.6	84.6	84.6	84.6		-
Net power plant output (MW _{el})	567.3	571.1	449	447	435	457	451	525.3	-
Net plant efficiency (% LHV)	37.8	38.0	31.2	31.1	30.3	31.8	31.4	-	-

^a Based on IEAGHG report but revised and evaluated for consistent comparison in this work (Corden et al., 2014)

^b This work for a high CO₂ purity case only studied the CPU system

^c The Air Liquide process uses an alternative low temperature distillation method for removal of SO_x, NO_x. A portion of the CO₂ product is pumped from the cold box conditions (rather than full vaporisation / compression used in other processes)

^d The Praxair process exceeds 100ppm O₂ in product stream and is therefore not considered to meet EOR specifications

Table 6 shows the CPU power consumed for the systems compared, which vary from 114 to 194 kWh/tCO₂. These differences can be explained by the different process configurations used, and the variation in achieved unit performance with respect to CO₂ purity and recovery.

In particular, the selection of process operating pressures imposes differing penalties, since streams must be compressed to enable condensation, depressurised to provide cooling in the cold box, and then re-compressed as required for CO₂ storage. The system presented in this work follows the principles of the low temperature CO₂ recovery process proposed in a Costain patent application (Corden et al., 2012) in which CPU cooling requirements are matched by splitting and depressurising product streams to different pressure levels.

Of those listed in Table 6, the systems proposed in this work, the Air Products case at 30 bar, the Air Liquide case, and the Posch and Haider (2012) case are capable of delivering a CO₂ product with an oxygen concentration of 100 ppm or less for the purified CO₂ stream.

The CPU power requirements of the current work sit between those reported for the Air Products and Air Liquide systems. The Air Liquide system benefits from a partially pumped product stream and the recycle of expanded inert streams to provide cooling. The system proposed in Posch and Haider (2012) provides cooling by reducing the whole CO₂ stream to a low pressure level of 5.8 bar, with increased penalties.

For the high CO₂ purity (>99%) illustrative cases shown here, the Costain process in this work shows the highest CO₂ removal efficiency of 90%.

It should, of course, be noted that all vendors are continuously developing their technology offerings and are likely to be able to offer a range of different CO₂ capture solutions that strike different balances among key factors such as CO₂ purity, CO₂ recovery rate, product specifications, transport system requirements and cost depending on customer needs.

3.2 Summary of heat integration and plant thermal efficiency results

121.4 MW_{th} was added to the steam cycle from the CPU and ASU, and 15.5 MW_{th} was removed from the cycle for the purpose of providing heat for dehydration units in the CPU and ASU, and for heating the vent stream exiting the CPU. The net balance of heat to the steam cycle as a result of the integration was therefore 105.9 MW_{th}. Table 6 shows that the specific power consumption for the studied CPU system was 0.435 GJ_{el}/tCO₂ (120.9 kWh/tCO₂) after

heat integration between the steam cycle and CPU. This is within those reported for Air Liquide, Air Products and Praxair patent cases for delivering a high purity CO₂ product (>99%).

A net plant efficiency of 38.02% was found in this work, as detailed in Table 6. This is 0.3%-points higher than the reference IEAGHG 2005/9 case, while providing a higher purity CO₂ product. The absolute efficiencies derived in this work are a function of the design basis. The study scheme adopted from the IEAGHG 2005/9 report includes a number of features that result in higher values than would otherwise be expected:

The absence of an FGD, and the assumption that NO_x and SO_x will be removed during flue gas compression allows for the use of flue gas feedwater heaters in the steam cycle, which would not be possible at the outlet of a wet FGD unit. A number of simplifications and omissions in the original study were acknowledged and reviewed (Corden et al., 2014), for example system pressure drop is understated in the IEAGHG 2005/9 report but this was acknowledged and accepted for other study cases, to give a consistent approach.

In contrast to the IEAGHG 2005/9 report, this study employs flue and product gas compression trains with a higher number of intercooled stages, decreasing the energy penalty in the CPU but also decreasing the gross plant efficiency due to reduced quantities of heat available for integration between the CPU compression train and the steam cycle. Our analysis, detailed in Corden et al. (2014), suggests that maximising high-temperature heat integration between compression intercooling and the steam cycle does not necessarily offer any efficiency or cost benefit compared to an optimised low temperature scheme; it is not clear that configurations with fewer compression stages, which tend to have higher grade heat available for integration due to increased temperatures at the exit of compressor stages, but also higher compression duties, necessarily provide net efficiency increases. The integrated solution for low temperature, more conventional compression equipment and associated heat exchangers offers potential for process simplification, particularly considering interfaces between the steam cycle and the CPU. This provides an opportunity to develop safer and more reliable plants. These results challenge previously published assumptions that an optimised integrated process would be based on high temperature integration from compression trains.

The relative increase in efficiency between similar cases can be attributed to the extensive power plant integration scheme and optimisation within the novel CPU. This increase is considered significant and can be used as a basis for further investigations.

4. Conclusions

This study presents a novel configuration of a CPU process, extensively integrated with an oxycoal combustion plant, to provide high purity CO₂ streams at 90% capture efficiency with a net plant efficiency of 38.02% (LHV). These values are promising and comparable with those found for oxycoal combustion plant in the literature, including (but not limited to) those providing high purity CO₂. For example, this work shows an improvement in plant efficiency of 0.3 %-points was seen from our simulated oxyfuel base case, a case that only provided 95.5% CO₂ purity compared with the >99% purity of the improved case presented here. The improvements for this work can be attributed to the power plant integration scheme, designed for maximum energy efficiency, and the optimised CO₂ recovery unit. The CPU was modelled in detail in order to deliver a high purity CO₂ product (>99%) with an oxygen level limited to 100 ppm, for potential EOR applications. External sinks and heat sources in the steam cycle and CPU compression were also identified and integrated.

The current study was constrained to steady state analysis. The model created for this study, combined with the knowledge gained from integration work forms a basis for further analysis. Future work is anticipated for system control and transient/part load operation, since non-steady state analysis remains essential to understanding performance over the full anticipated operating range of a CCS power station. Further work is also required to examine restrictions or practical constraints that would set the final design of the integration approach.

Acknowledgement: The scientific work was supported by DECC CCS Innovation Programme (2012) “OXYPROP – Oxyfuel Penalty Reduction Programme”.

References

- Abbas, Z., Mezher, T., Abu-Zahra, M.R.M., 2013. CO₂ purification. Part I: Purification requirement review and the selection of impurities deep removal technologies. *Int. J. Greenhouse Gas Control* 16, 324-334.
- Allam, R.J., 2008. Purification of carbon dioxide. United States Patent, Air Products, US 7416716B2
- Besong, M.T., Maroto-Valer, M.M., Finn, A.J., 2013. Study of design parameters affecting the performance of CO₂ purification units in oxy-fuel combustion. *Int. J. Greenhouse Gas Control* 12, 441-449.
- Boot-Handford, M.E., Abanades, J.C., Anthony, E.J., Blunt, M.J., Brandani, S., Mac Dowell, N., Fernandez, J.R., Ferrari, M.-C., Gross, R., Hallett, J.P., Haszeldine, R.S., Heptonstall, P., Lyngfelt, A., Makuch, Z., Mangano, E., Porter, R.T.J., Pourkashanian, M., Rochelle, G.T., Shah, N., Yao, J.G., Fennell, P.S., 2014. Carbon capture and storage update. *Energy Environ. Sci.* 7, 130-189.

- Corden, C., Chalmers, H., Errey, O., Font Palma, C., Porter, R., Taylor, M., Jackson, S., Livesey, V.B., Elliff, B., 2014. OxyPROP - Oxyfuel Penalty Reduction Option Programme. Department of Energy & Climate Change. CCS Innovation Programme (2012). Ref: 7564-0200-075-07-1005-001 REV O
- Corden, C., Eastwood, T.D., Finn, A.J., 2012. Process and Apparatus for Purification of Carbon Dioxide, in: PCT/GB2012/050421, PCT/GB2012/050423, PCT/GB2012/050422. COSTAIN Oil, Gas & Process Limited, GB.
- de Visser, E., Hendriks, C., Barrio, M., Mølnvik, M.J., de Koeijer, G., Liljemark, S., Le Gallo, Y., 2008. Dynamis CO₂ quality recommendations. *Int. J. Greenhouse Gas Control* 2, 478-484.
- de Visser, E., Hendriks, C., de Koeijer, G., Liljemark, S., Barrio, M., Austegard, A., Brown, A., 2007. D.3.1.3 DYNAMIS CO₂ quality recommendations, Towards Hydrogen and Electricity Production with Carbon Dioxide Capture and Storage. Ecofys Netherlands b.v.
- Dillon, D.J., White, V., Allam, R.J., Wall, R.A., Gibbins, J., 2005. Oxy Combustion Processes for CO₂ Capture from Power Plant. IEA Greenhouse Gas R&D Programme, p. 212.
- DOE/NETL, 2012. Quality Guidelines for Energy System Studies. CO₂ Impurity Design Parameters. DOE (United States Department of Energy)/NETL (National Energy Technology Laboratory).
- Font Palma, C., Martin, A.D., 2013. Model based evaluation of six energy integration schemes applied to a small-scale gasification process for power generation. *Biomass Bioenergy* 54, 201-210.
- Koottungal, L. 2014. 2014 worldwide EOR survey - Special report. *Oil Gas J.*
- Kuuskräa, V., 2013. The role of enhanced oil recovery for carbon capture, use, and storage. *Greenhouse Gas Sci. Technol.* 3, 3-4.
- Metz, B., Davidson, O., de Coninck, H., Loos, M., Meyer, L., 2005. IPCC Special Report on Carbon Dioxide Capture and Storage. Intergovernmental Panel on Climate Change (IPCC), New York, NY, USA.
- Pipitone, G., Bolland, O., 2009. Power generation with CO₂ capture: Technology for CO₂ purification. *Int. J. Greenhouse Gas Control* 3, 528-534.
- Posch, S., Haider, M., 2012. Optimization of CO₂ compression and purification units (CO₂CPU) for CCS power plants. *Fuel* 101, 254-263.
- Serpa, J., Morbee, J., Tzimas, E., 2011. Technical and Economic Characteristics of a CO₂ Transmission Pipeline Infrastructure. European Commission Joint Research Centre, Petten, Netherlands.
- Strube, R., Manfrida, G., 2011. CO₂ capture in coal-fired power plants—Impact on plant performance. *Int. J. Greenhouse Gas Control* 5, 710-726.
- Wall, T., Stanger, R., Santos, S., 2011 Demonstrations of coal-fired oxy-fuel technology for carbon capture and storage and issues with commercial deployment. *Int. J. Greenhouse Gas Control* 5, Supplement 1, S5-S15.
- Wetenhall, B., Race, J.M., Downie, M.J., 2014. The Effect of CO₂ Purity on the Development of Pipeline Networks for Carbon Capture and Storage Schemes. *Int. J. Greenhouse Gas Control* 30, 197-211.
- White, V., Wright, A., Tappe, S., Yan, J., 2013. The Air Products Vattenfall Oxyfuel CO₂ Compression and Purification Pilot Plant at Schwarze Pumpe. *Energy Procedia* 37, 1490-1499.